Quantitative X-Ray Phase Analysis and EPR Spectra in the System Y$_2$BaCuO$_5$–YBa$_2$Cu$_3$O$_{6+x}$

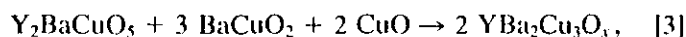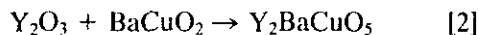F. Hanic,[1] G. Plesch,* Š. Buchta, J. Dobrovodský, and L. Danielik

*Institute of Inorganic Chemistry, Slovak Academy of Sciences, 842 36 Bratislava, Slovakia; and *Department of Inorganic Chemistry, Faculty of Natural Sciences, 842 15 Bratislava, Slovakia*

The quantitative phase analysis in the system Y$_2$BaCuO$_5$(2–1–1)–YBa$_2$Cu$_3$O$_{6+x}$(1–2–3) was performed by the X-ray powder diffraction (XRPD) method based on the comparison of the integral intensities of the X-ray diffractions of the investigated system with the corresponding intensities of standard mixtures of (2–1–1) and (1–2–3) components of known composition. To avoid the orientation effects of the (1–2–3) components, the selected mixtures were homogenized by the admixture of 50 mass% α-Al$_2$O$_3$. The constituent (2–1–1) showed no preferential orientation, neither in the bulk textured materials prepared by the quench and melt growth technique, nor in the samples ground to powder. The X-ray diffraction results were in accordance with the semiquantitative estimation of the concentration of the paramagnetic (2–1–1) phase obtained from the results of EPR measurements on powdered samples. On the other hand, the intensity of the EPR spectra strongly decreased in bulk materials due to the skin effect. The electric conductivity of (1–2–3) at room temperature causes the microwave fields to penetrate to a depth of approximately 10 μm, which is the only EPR active region. © 1995 Academic Press, Inc.
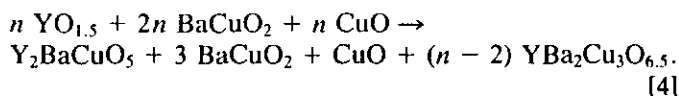
1. INTRODUCTION

The "green phase," Y$_2$BaCuO$_5$ (2–1–1), is an important constituent of the system Y–Ba–Cu–O. It may accompany the superconducting YBa$_2$Cu$_3$O$_{6+x}$ (1–2–3) phase even in the case where a stoichiometric reactant mixture YO$_{1.5}$: BaCO$_3$: CuO = 1 : 2 : 3 was used for the synthesis. The appearance of the (2–1–1) phase in such case indicates that the reaction, consisting of three consecutive steps (1),

$$BaCO_3 + CuO \rightarrow BaCuO_2 + \nearrow CO_2 \quad [1]$$

$$Y_2O_3 + BaCuO_2 \rightarrow Y_2BaCuO_5 \quad [2]$$

$$Y_2BaCuO_5 + 3\ BaCuO_2 + 2\ CuO \rightarrow 2\ YBa_2Cu_3O_x, \quad [3]$$

stopped at some $n -$ value of the reacting system:

$$n\ YO_{1.5} + 2n\ BaCuO_2 + n\ CuO \rightarrow$$
$$Y_2BaCuO_5 + 3\ BaCuO_2 + CuO + (n - 2)\ YBa_2Cu_3O_{6.5}.$$
$$[4]$$

The kinetic study of the solid state reaction [3] showed that the process proceeds by a three-dimensional reaction mechanism, in which Ba^{2+} and Cu^{2+} particles diffuse across the growing (1–2–3) shell into the unreacted core of (2–1–1). The reaction takes place at the reaction zone. With time t, the product layer shell increases, while the unreacted core shrinks progressively (the unreacted-core-shrinking model) (1). The diffusion of Ba^{2+} and Cu^{2+} ions across the growing (1–2–3) shell becomes slower and finally it stops at some value of n where the reaction time is not sufficient for reaction completion.

In the case of the quench and melt texturing technique for preparation of dense textured bulk samples, the "green phase" is formed as a result of cooling down the system Y$_2$O$_3$ + liq (4 BaO + 6 CuO), which exists above the peritectic temperature $T_p = 1015$°C (2, 3):

$$Y_2O_3 + liq\ (4\ BaO + 6\ CuO) \rightarrow$$
$$Y_2BaCuO_5 + liq\ (3\ BaO + 5\ CuO). \quad [5]$$
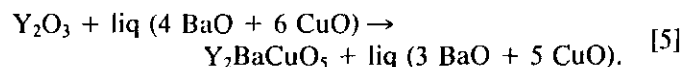
On slow cooling below the peritectic temperature, the system [5] converts to a layered structure of YBa$_2$Cu$_3$O$_x$ (2, 3):

$$Y_2BaCuO_5 + liq\ (3\ BaO + 5\ CuO) \xrightarrow{\ 1000°C\ } 2\ YBa_2Cu_3O_x. \quad [6]$$
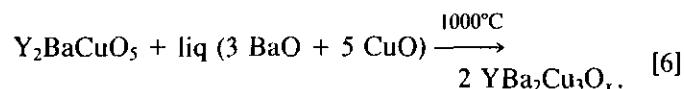
The pinning energy U_p of the melt-textured bulk (1–2–3) with (2–1–1) inclusions was found to be increased by an order of magnitude in comparison with pure (1–2–3) (5). In other words, strong pinning centers of high density, which are in the form of nonsupercon-

ducting admixtures, must be introduced into a superconductor in order to achieve high J_c values.

A controlled amount of (2–1–1) can be also incorporated by postannealing of the system (1–2–3)–(2–1–1) between 900 and 1020°C (4). The optimal amount of (2–1–1) admixture lies in the range 10–20 vol% (2, 3). Due to incomplete peritectic reaction [6], even after slow cooling, the textured solid product $YBa_2Cu_3O_{6+x}$ contains randomly distributed Y_2BaCuO_5, CuO, and $BaCuO_2$, frequently in the form of an amorphous solid.

Quantitative X-ray powder diffraction (XRPD) analysis was used in this work to detect and quantify the crystalline phases in the system Y_2BaCuO_5–$YBa_2Cu_3O_x$. However, it cannot detect and specify amorphous phases having grain sizes less than 50 Å. This was why we also applied the EPR method, which allows detection of paramagnetic phases regardless of their crystallinity.

2. EXPERIMENTAL

The dense textured $YBa_2Cu_3O_{6.9}$ material was prepared by the quench and melt growth (QMG) technique in a two-step process (2, 3). In the first step a melt of the Y : Ba : Cu = 1 : 2 : 3 system was quenched from 1400°C on a copper plate. The product was ground, pressed into pellets, and then, in the second step, slowly cooled from 1100°C to room temperature in an oxygen atmosphere, rendering a textured $YBa_2Cu_3O_{6.9}$ as a final product. The preparation, microstructure, and electrical properties of the obtained product were described in detail in Ref. (7).

The compounds used to construct a calibration curve for quantitative XRPD analysis were $YBa_2Cu_3O_{6.9}$ and Y_2BaCuO_5. The (1–2–3) phase was prepared by the standard citrate method (8). The (2–1–1) constituent was synthesized from the corresponding oxides at 950°C in oxygen (9). The phase purity of the obtained product was controlled by XRPD analysis. The values of x in $YBa_2Cu_3O_x$ were determined from the known dependence of the unit cell parameters of (1–2–3) on x (10).

The XRPD patterns were taken on a Philips 1540 diffractometer using $CuK\alpha$ radiation. The powdered samples were mixed with 50 mass% of α-Al_2O_3. This substance, with spheroidal particles, effectively avoids the striking orientation effects which were observed even in the finely powdered (1–2–3) phase. The constituents were sifted on a set of sieves to separate finer particles (below 10^{-4} cm) from coarser ones, which were reground and homogenized with the finer portion.

The EPR spectra were measured on a Varian E-4 instrument in the X-band at room temperature. A semiquantitative estimate of the number of spins was based on the comparison of signal amplitudes of the measured and standard samples. This very simple method can be used when the sample and the standard have lines of similar width and shape. In this case the amount of paramagnetic phase is directly proportional to the signal amplitude. A mixture of 27.5 mass% Y_2BaCuO_5 with 72.5 mass% $YBa_2Cu_3O_{6.9}$ was used as standard. Since this method is semiquantitative, we estimate the relative mass concentration error as ±20%.

3. RESULTS AND DISCUSSION

3.1. X-Ray Diffraction Analysis

The XRPD analysis was performed with the help of standard mixtures of powders of known composition containing an admixture of the reference phase α-Al_2O_3. The system, containing ω_1 mass% of the first constituent (2–1–1), ω_2 mass% of the second constituent (1–2–3), and ω_3 mass% of the calibration standard (α-Al_2O_3), can be evaluated from the chosen integral intensities of the diffraction lines I_1 and I_2 of the constituents and I_3 of the reference line of the standard (the chosen diffractions do not interfere with other diffractions) by a system of three equations (11):

$$I_1/I_2 = (B_1/B_2) \cdot (\omega_1/\omega_2); \quad I_2/I_3 = (B_2/B_3) \cdot (\omega_2/\omega_3); \quad [7]$$

$$\omega_1 + \omega_2 + \omega_3 = 1. \quad [8]$$

In general the measurements of p selected intensities I_{ij}^0 in the i calibration samples ($i = 1, 2, \ldots p$), each consisting of three components ($j = 1, 2, 3$), in which the fractional mass concentrations ω_{ij} are known, allow evaluation of proportions of experimental constants B_j, i.e., $B_2 : B_1$ and $B_3 : B_1$, and their replacement by the expressions

$$\omega_{i1} = \sum_{i=1}^{p_1} I_{i1} \Big/ \sum_{i=1}^{p_1} I_{i_01} \quad [9a]$$

$$\omega_{i2} = \sum_{i=1}^{p_1} I_{i2} \Big/ \sum_{i=1}^{p_1} I_{i_02}. \quad [9b]$$

I_{i_0j} are intensities of the pure constituent phase j related to the sets of intensities I_{ij} ($j = 1, 2$, and $3; i = 1, 2, \ldots, p_j$) all taken under identical conditions. The standard mixtures were prepared under the following conditions:

$$\omega_{i2} = 1 - \omega_{i1}; \quad (\omega_{i1} + \omega_{i2})/\omega_{i3} = 1. \quad [10]$$

The fractional mass concentrations ω_{i1} acquired the following values: 1, 0.6885, 0.3443, 0.2754, 0.2065, 0.1721, 0.1377, 0.1033, 0.0688, 0.0344, and 0.0172 (the component Y_2BaCuO_5).

Figure 1 shows the plots of ω_{i1} vs $\sum_{i=1}^{p_1} I_{i1}/\sum_{i=1}^{p_1} I_{i_01}$ and ω_{i2} vs $\sum_{i=1}^{p_2} I_{i2}/\sum_{p=1}^{p_1} I_{i_02}$ for Y_2BaCuO_5 and $YBa_2Cu_3O_{6.9}$
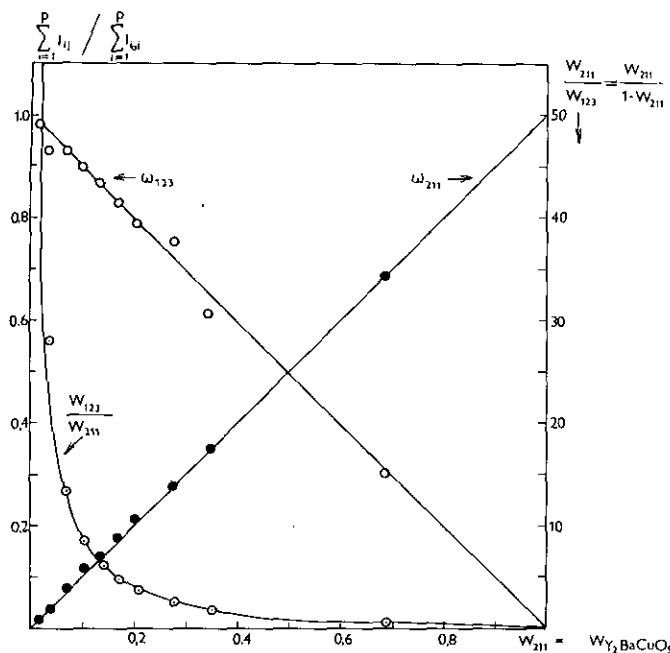
FIG. 1. Dependence of the mass fraction ω_{ij} (solid line) on $\Sigma_{i=1}^{p} I_{ij}/\Sigma_{i=1}^{p} I_{i0j}$ experimental points (j = 1 or 2 for Y_2BaCuO_5 and $Y Ba_2Cu_3O_x$ components, respectively). The full curve represents the standard proportion ω_{i1}/ω_{i2} and experimental points are given by (ΣI_{i2} $\Sigma I_{i01})/(\Sigma I_{i1} \Sigma I_{i02})$. I_{ij} are integral intensities of XRPD.

attempted a semiquantitative estimate of its concentration by EPR spectroscopy. According to the results of EPR measurements on powdered samples the (211) phase was admixed in the amount of 18.0 mass%. This value is in excellent agreement with the value of 17.2 mass% obtained from the quantitative XRPD phase analysis. On the other hand, measurements on bulk samples yielded EPR spectra with distinctly lower intensity, which corresponded to only ~1.5 mass% of the green phase.

To explain these significant differences between the intensities of the EPR spectra of the bulk and powdered samples, we prepared series of $Y_2BaCuO_5/YBa_2Cu_3O_{6.9}$ mixtures, which were pelletized and sintered in oxygen at 950°C.

In the above mixtures, which were ground after sintering, the amplitude of the EPR signal was proportional to the admixture of the "green phase" (Table 1). When a semiquantitative estimate of the number of spins (concentration of the "green phase") was attempted, we realized that more reliable results were obtained when a mixture of Y_2BaCuO_5 with $YBa_2Cu_3O_{6.9}$ was used as a standard instead of the pure green phase. $YBa_2Cu_3O_{6.9}$ is a conductor at room temperature and strongly lowers the Q-factor of the microwave cavity. Generally, if we compare signal intensities, it is necessary to take samples with comparable electric properties and volume to perform approximately equal field perturbation in the cavity.
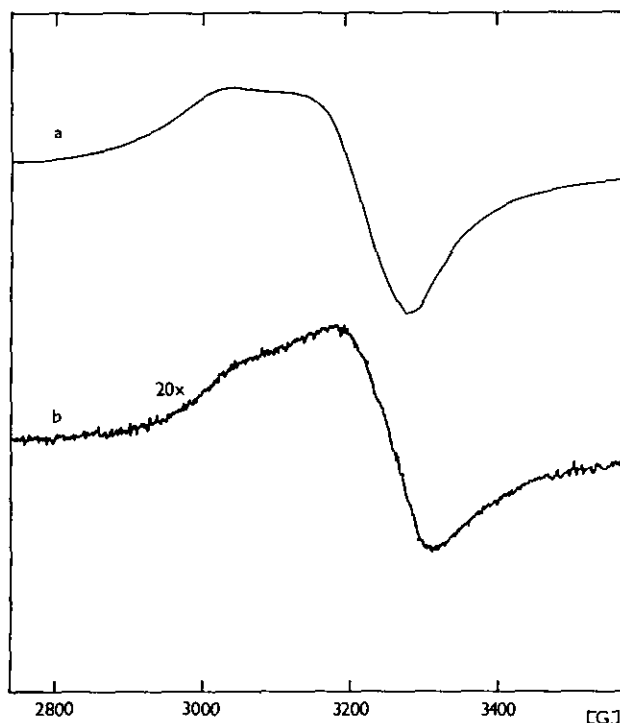
respectively, which reflect good agreement between the fractional mass concentrations ω_{ij} (full line) and the intensity fractions $\Sigma I_{ij}/\Sigma I_{i0j}$ (experimental points). The full curve in Fig. 1 corresponds to the proportion of the fractional concentrations ω_{i1}/ω_{i2} of Y_2BaCuO_5 and $YBa_2Cu_3O_{6.9}$, the experimental points are calculated from the background subtracted integral intensities according to [9]. For Y_2BaCuO_5 the intensities of 131, 211, 002, and 142 diffractions were applied; for $YBa_2Cu_3O_{6.9}$ the intensities of 003, 013, 103, 113, 006, 200, and 123 were included. The concentration of (2-1-1) in the (1-2-3) ceramic compact prepared by the QMG technique was evaluated from the intensity data taken from the powdered sample with an admixture of 50 mass% of α-Al_2O_3, applying the standard curve for ω_1/ω_2 in Fig. 1 as well as the normalization condition [10]. The relations [9] were used. The concentration thus obtained was 17.2(6) mass% of (2-1-1) in (1-2-3).

3.2. EPR Spectra

The Y–Ba–Cu–O textured superconductor prepared by the QMG technique showed an axial EPR spectrum with the g values $g_\perp$ = 2.06 and $g_\parallel$ = 2.22 (Fig. 2). This spectrum can be ascribed to the admixture of the "green phase" in the EPR silent matrix of $YBa_2Cu_3O_{6+x}$ (12). However, remarkable effects were observed when we

FIG. 2. EPR spectrum of samples containing 17.2 mass% of green phase in $YBa_2Cu_3O_{6.9}$: (a) powdered sample; (b) bulk sample.

TABLE 1
EPR Analysis of the Content of Green Phase in Y_2BaCuO_5/$YBa_2Cu_3O_{6.9}$ Mixtures

Admixed mass% of Y_2BaCuO_5	Percentage of Y_2BaCuO_5 estimated from EPR (mass%)[a]		
	Before sintering	Sintered sample ground to powder	Sintered bulk sample
1.7	1.7	1.5	—
3.4	2.9	2.2	—
10.3	10.2	6.2	0.4
17.2	15.9	17.8	0.5
20.7	22.9	20.9	0.7
68.8	72.3	64.3	65.8

Note. A standard containing 27.5 mass% of green phase and 72.5 mass% of $YBa_2Cu_3O_{6.9}$ was used.

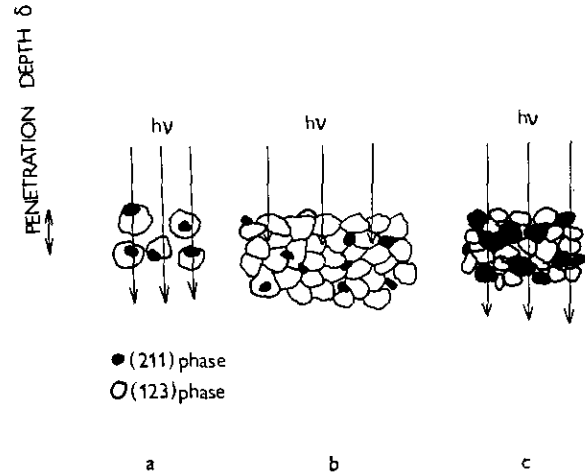[a] Estimated deviation ±20 rel. mass%.

FIG. 3. Scheme of penetration of microwaves into (a) powdered sample, (b) bulk sample with low content of green phase, (c) bulk sample with high content of green phase.

● (211) phase
○ (123) phase

Remarkable results were obtained when we compared the EPR spectra of the bulk samples of size ~2 × 2 × 2 mm with those of powdered samples. The amplitudes of the signals belonging to the bulks decreased in such a way that the signal of the two samples with the lowest content of green phase was below the noise level (Table 1). In the samples with intermediate concentrations of Y_2BaCuO_5 the amplitude of the signal of the bulks decreased by more than one order of magnitude in comparison with the signal of the corresponding powdered sample (Table 1). On the other hand, in samples containing a high portion of paramagnetic admixture, the intensity of the signal corresponded to the actual content of the green phase both in powder and in bulk (Table 1). These results can be explained by the electromagnetic shielding of the inner part of the sample due to the skin-effect. The microwave field penetrates only into a limited depth of a conductor δ, which is given by

$$\delta = (\pi f \sigma \mu)^{-1/2}, \qquad [11],$$

where f is the frequency of the field and σ and μ are the conductivity and permeability of the material, respectively.

For X band frequency (9 GHz) and typical resistivity ($\rho \sim 10^{-4}$ Ω cm) in $YBa_2Cu_3O_{6.9}$, δ is approximately 10 μm (14) and exceeds the geometrical dimensions of the grains in the powdered sample. However, the conducting grains are electrically connected in sintered samples and consequently the inner part is effectively shielded in the microwave frequency band. In samples with higher concentrations of the Y_2BaCuO_5 phase, the intergrain connections are disturbed and microwave field completely penetrates the sample and the whole amount of the green phase becomes EPR active (Fig. 3).

The influence of the electric properties of the sample on the signal intensity can be nicely demonstrated by the series of sintered $YBa_2Cu_3O_x$ powders, which contained ~2.5 mass% of the green phase. Their electrical conductivity was varied by changing the oxygen content by quenching from temperatures 350–850°C. The oxygen content decreased with increasing quenching temperature (x changed from 6.9 to 6.4) (13). Simultaneously the sample changed from a conductor at room temperature to an insulator. Even when all these samples contained the same amount of "green phase," the amplitude of the EPR signal remarkably increased with decreasing electrical conductivity of the sample.

The shape of the EPR line slightly varies for samples with different amounts of the Y_2BaCuO_5 admixture. In case where the whole bulk is EPR active (powders or pellets with high concentration of dielectric admixture) the spectrum does not substantially differ from the green phase standard (Fig. 2A). The EPR lineshape in bulk samples is asymmetric (Fig. 2B). When a layer of a thickness of about 0.2 mm, which surely exceeds the skin depth, was removed from both sides of the pellet, the powder from the original surface showed a typical axial spectrum of the pure green phase. On the other hand, the shape of the EPR spectrum of the remaining part of the bulk sample was again asymmetric. This can be explained by the fact that for metallic samples with characteristic size exceeding the skin depth, the EPR line shape becomes asymmetric due to exchange interaction between conducting electrons and localized magnetic moments (14).

CONCLUSIONS

1. The quantitative phase analysis of the ceramic compact $YBa_2Cu_3O_{6+x}$, containing intergrain admixtures of Y_2BaCuO_5 is of considerable importance, since this admixture promotes flux pinning in superconductors. The quantitative XRPD analysis of the compact ($YBa_2Cu_3O_{6+x}$ + Y_2BaCuO_5) prepared by the QMG technique is rather inaccurate, since the $YBa_2Cu_3O_{6+x}$ matrix is textured to a high degree. A preferred orientation also remains in powdered samples. An effective way of supressing these effects is grinding the ceramic bulk and preparing a homogenous mixture diluted with α-Al_2O_3 1:1. The α-Al_2O_3 admixtur also operates at the same time as an inner standard. An effective method for analyzing such powder XRPD patterns is presented.

2. EPR spectroscopy can be effectively used for semiquantitative estimation of the concentration of EPR active Y_2BaCuO_5 in the EPR silent $YBa_2Cu_3O_{6+x}$ matrix. However, mainly the intensity of the EPR spectra and to some extent also their shape are distinctly influenced by the electrical properties of the matrix. These effects are caused by modification of the penetration depth of microwaves into the sample by conduction electrons (skin effect). For correct interpretation of the EPR spectral data these influences must be taken in account. The comparable size of granulae is of great importance. The use of the EPR method is limited to paramagnetic compounds with sufficiently narrow EPR lines which are distributed in an EPR silent matrix. For example, we could not detect CuO and $BaCuO_2$, which according to equation [4] are also present in the $YBa_2Cu_3O_{6+x}$ samples prepared by QMG, by EPR. The first admixture is EPR silent and the second one has a very broad EPR line, which vanishes in the baseline.

3. The XRPD and EPR methods are complementary in some special cases. For example, in rapidly quenched precursor in the first step of the QMG procedure according to reaction [5], Y_2BaCuO_5 remains in a noncrystalline state, which cannot be seen by XRPD, but is readily detected by EPR.

REFERENCES

1. Nae-Lih Wu, Ta-Chin Wei, Shau-Y Hou, and S-Yen Wong, *J. Mater. Res.* **5**, 2056 (1990).
2. M. Murakami, *Supercond. Sci. Technol.* **5**, 185 (1992).
3. K. Salama, V. Selvamanickam, and D. F. Lee, "Processing and Properties of High Temperature Superconductors" (S. Jin, Ed.), World Scientific, Singapore, 1992.
4. T. Yamamoto, S. K. Chan, M. Strubicar, T. R. S. Prasanna, and R. C. O. Handley, *Mater. Lett.* **10**, 243 (1991).
5. L. T. Sagdahl, T. Laegrid, H. Fossheim, M. Murakami, H. Fujimoto, S. Gotok, K. Yamaguchi, H. Yamauchi, K. Koshizuka, and S. Tanaka, *Physica C* **172**, 495 (1991).
6. M. Murakami and T. Matsushita, *ISTEC J.* **3**, 21 (1990).
7. F. Hanic, Š. Buchta, L. Danielik, F. Gömöry, G. Plesch, and S. Valtýniová, *Condens. Mater. Mater. Commun.* **1**, 63 (1993).
8. F. Hanic, M. Polák, F. Gömöry, G. Plesch, I. Horváth, P. Lobotka, and Ĺ. Gáliková, *Br. Ceram. Trans. J.* **88**, 35 (1989).
9. H. Fjellvag, P. Karen, and A. Kjekshus, *Acta Chem. Scand. A* **41**, 233 (1993).
10. L. A. Muradyan, V. N. Molchanov, R. A. Tamazyan, and V. I. Simonov, *Physica C*, **162–164**, 536 (1989).
11. J. Fiala, *Silikáty* **29**, 273 (1985).
12. G. Plesch, F. Hanic, B. Švecová, Š. Buchta, L. Danielik, J. Dobrovodský, and D. Reinen *Mol. Phys. Rep.* **5**, 119 (1994).
13. W. E. Farneth, R. K. Bordia, E. M. McCarron, M. K. Crawford, and R. B. Flippen, *Solid State Commun.* **66**, 953 (1988).
14. I. Garifullin, N. N. Garif'yanov, N. E. Alekseevskii, and F. Kim, *Physica C* **179**, 9 (1991).